WASTE HEAT RECOVERY FROM DIESEL ENGINE USING CUSTOM DESIGNED HEAT EXCHANGER AND THERMAL STORAGE SYSTEM WITH NANOENHANCED PHASE CHANGE MATERIAL

by

Maria Robert WILSON JOHN[a*], Abhishek Kumar SINGH[a], Abhinay Kumar SINGH[a], and Lalgudi Ramachandran GANAPATHY SUBRAMANIAN[b]

[a] Department of Mechanical Engineering,
Dr. M. G. R. Educational and Research Institute, Chennai, India
[b] Aerospace Engineering, School of Mechanical Engineering,
SRM University, Chennai, India

Original scientific paper
DOI: 10.2298/TSCI160426264W

In this research study an attempt has been made to recover the heat energy of the exhaust gas from a Diesel engine, using a triangular finned shell and tube heat exchanger with segmental baffle at 20°, and efficiently store as sensible and latent heat energy using thermal storage tank having phase change material with CuO nanoparticles. The nanoparticles and the phase change material form the nanoparticle-enhanced phase change material and mainly the thermal conductivity of the phase change material can be enhanced through the dispersion of the nanoparticles. The temperature variations of the heat transfer fluid in the heat recovery heat exchanger with various load conditions of the Diesel engine are studied. The performance of the heat exchanger is evaluated using heat extraction rate and effectiveness. Evaluation of the performance of the thermal storage system can be analyzed by using the total heat energy stored and charging rate during the charging period for the selected nanoparticle-enhanced phase change material.

Key words: *baffle, heat recovery heat exchanger, phase change material, thermal storage system, nanoparticles*

Introduction

Energy is a primary source for the development of any country. Since the last few decades, United States, China, and Russia have continued to be the main three largest energy consumers in the world followed by India in the fourth place. Energy conservation refers to reducing energy losses that in turn translate to less consumption of engine fossil fuel. Internal combustion (IC) engines are the major consumers of fossil fuel around the globe [1]. Generally, the IC engine eliminates nearly 40% of the heat energy through the exhaust [2]. If the exhaust heat of the IC engines can be recovered, then the efficiency of the engine will be increased [3]. Moreover, global warming also will be reduced [4]. In India, a majority of vehicles are still powered either by petrol engines or by Diesel engines. Diesel engines are more widely used in many industries than petrol engines due to their abilities and advantages for

* Corresponding author, e-mail: mrwjohn2011@gmail.com

producing in-situ energy, electricity, transportation, *etc.* However, the inherent drawback of Diesel engines is that a large amount of their fuel energy is wasted through the exhaust [5]. Researchers confirm that more than 30-40% of fuel energy is wasted from the exhaust and only 12-15% of the fuel energy is converted into useful work [6, 7]. Many researches confirmed that the waste heat recovery (WHR) from an engine exhaust has the ability to cut lower fuel consumption without increasing the engine emissions, and new technological advancements have not only made these systems possible but also cost-effective [8, 9].

Exhaust gas heat energy from Diesel engines can mostly be effectively recovered by using suitable heat exchangers. The heat exchanger is a device used to influence the process of heat exchange between two or more fluids at different temperatures. Heat exchangers are intensely used in various energy transfer applications, such as refrigeration and air-conditioning systems, thermal power plants, automobile industries, chemical processing industries, cryogenic industries, and space or aeronautical applications [10]. Many types of heat exchangers are available to recover the heat from the exhaust gas of the IC engine. Shell and tube type heat exchangers are more popular in industrial applications because of its reliability and high heat transfer effectiveness. Hatami *et al.* [11] have presented a short review of different WHR technologies in engines such as thermo-electric generators (TEG), organic Rankine cycle (ORC), 6-stroke engines, turbocharging, exhaust gas re-circulation (EGR), and exhaust heat exchangers. They have also given a complete review of different heat exchangers' designs for maximizing the exhaust WHR of Diesel engines. Bari and Hossain [12] were able to recover enough waste heat to produce 23.7% additional power from the exhaust of a Toyota 13B Diesel engine by optimizing the design of shell and tube heat exchangers in the Rankine cycle. They also optimized the working fluid pressure and orientation of the heat exchangers. Morcos [13] studied the heat transfer and fluid flow characteristics of shell and dimpled tube heat exchangers used for WHR. Morcos found that an additional 10% of the maximum brake power could be developed by exhaust heat recovery in a Diesel engine at a constant speed of 1500 rpm and tube Reynolds number of 8875 using the counter-flow of shell and dimpled tube heat exchangers.

The thermal performance of heat exchangers can be enhanced by heat transfer augmentation techniques, such as the use of fins. The main function of heat transfer augmentation techniques is to improve the thermal performance of a system by incrementing the surface heat transfer coefficient depending on the heat transfer coefficient that characterizes the base heat transfer surface. It is widely known that the heat transfer coefficient of the exhaust gas from an IC engine is much smaller than the functioning fluid heat transfer coefficient. As a consequence, fins are generally located on the exhaust gas side to enhance the heat transfer area [14]. Hatami *et al.* [15] theoretically analyzed finned type heat exchangers for IC engines exhaust WHR. The results showed that recovered heat can be improved by increasing the fin numbers and length where maximum heat recovery occurs in high engine load and speed. Ismail *et al.* [16] studied the solidification of phase change material (PCM) around a vertical axially finned isothermal cylinder, both theoretically and experimentally.

Baffles are one of the important pattern elements that can yield higher heat exchanger thermal performance and many improvements can be gained by varying the baffle configuration. Taher *et al.* [17] simulated the helical shell and tube heat exchangers with non-continuous helical baffles based on periodic boundaries using the commercial code of FLUENT. They reported that at the same mass flow rate, heat transfer per unit area, and pressure gradient decreased with the increase of baffle spaces. Elias *et al.* [18] studied the effect of different particle shapes (cylindrical, bricks, blades, and platelets) on shell and tube heat exchanger using different baffle angles and operated it with nanofluid. Elias *et al.* [18] concluded that the overall heat transfer coefficient, the heat transfer rate, and entropy minimization rate of cylindrical shape particles with 20° baffle angle were higher than 30°, 40°, and 50° baffle angles and segmental baffles with 1 vol.% concentration of Boehmite alumina (γ-AlOOH).

Thermal energy may be stored by three types of techniques such as: (1) sensible, (2) latent, and (3) thermo-chemical energy storage. The latent heat storage in a PCM has more desirable properties when compared to other heat storage systems due to its many useful features such as heat source at constant temperature, heat recovery with minimum temperature drop, low vapor pressure at working temperature, and chemical stability and non-corrosiveness [19]. Agyenim *et al.* [20], and Jegadheeswaran and Pohekar [14] presented a complete review of latent heat thermal energy storage (TES) systems using PCM. Sharma *et al.* [21] and Cunha and Emaes [22] reviewed TES for various applications using PCM. Pandiyarajan *et al.* [23] conducted experiments in a twin-cylinder Diesel engine to recover waste heat from the exhaust gas using rectangular finned shell and tube heat exchanger; a thermal storage system was used to store the available excess energy. Pandiyarajan *et al.* [23] also found that latent heat thermal storage systems are very desirable due to their high thermal storage capability and constant temperature performance during charging and discharging when compared with the sensible heat storage system. Nallusamy *et al.* [24] experimentally investigated the thermal behavior of a packed bed of combined sensible and latent heat TES unit integrated with constant temperature bath/solar collector. They concluded that the combined storage system gives better performance than the conventional sensible heat storage system.

The use of PCM in latent heat energy storage system is limited by low thermal conductivity [25]. Nanoparticles help to overcome this drawback because nanoparticles promote thermal conductivity of nanoenhanced phase change materials (NEPCM) compared to conventional PCM. Nanoparticles may be defined as the particles in the size range of 1-100 nm. There are five common shapes of nanoparticles available: cylindrical, bricks, blades, spherical, and platelets [17]. Hosseinizadeh *et al.* [26] theoretically analyzed the unconstrained dissolving of NEPCM within a globular vessel using RT27 with Cu particles as base material and nanoparticles. Their results showed that the nanoparticles improved the thermal conductivity of NEPCM compared to conventional PCM. The higher melting rate of NEPCM was achieved by improving the thermal conductivity and by reducing the latent heat of the storage system. Ranjbar *et al.* [27] investigated the heat transfer of a latent heat storage system containing NEPCM. They found that the suspended nanoparticles substantially increased the heat transfer rate and the nanofluid heat transfer rate also increased with an increase in the nanoparticles volume fraction. The experimental results of Jesumathy *et al.* [28] showed the thermal characteristics of paraffin wax embedded with nanosize CuO particles. The experimental results showed that the addition of CuO nanoparticles with paraffin wax improved the conduction and natural convection very effectively in composites and in paraffin wax.

From the afore-mentioned earlier research studies, it is concluded that the exhaust gas heat recovery with triangular finned shell and tube heat exchanger with segmental baffle and storage as sensible and latent heat energy using the thermal storage system with NEPCM has rarely been studied, so far. Thus, the researchers of the current study were motivated to work on various load conditions in a Diesel engine integrated with the custom designed heat exchanger and storage system with NEPCM for charging process. The study shows that it is one of best alternate heat recovery methods, with its improved thermal performance combined with thermal storage system.

Experimental set-up

The Diesel engine used in the current experiment is made by Kirloskar, India and has a 4-stroke, twin-cylinder, water cooled engine. The specifications of the Diesel engine are shown in tab. 1. An electrical dynamometer is attached to the Diesel engine for varying the loads. Schematic of the experimental set-up is shown in fig. 1. The arrangement consists of a triangular finned shell and tube heat exchanger with segmental baffles at 20°, an insulated cylindrical thermal storage tank with PCM and spherical CuO nanoparticles encapsulated cylindrical container to store the heat, an oil gear pump, an oil reservoir, and the Diesel engine. Normally the surface convective heat transfer coefficient of the exhaust gases will be very low and hence heat transfer surface on the exhaust gas side needs to have a much larger area for better heat transfer. This requirement can not be achieved by embedding the heat exchanger coil inside the storage tank. Hence, a separate heat exchanger is custom designed with finned tubes in which the exhaust gas is allowed to pass through the shell side to achieve a higher surface area of the gas side. The exhaust gas pipe of the Diesel engine is attached to the triangular finned shell and tube heat exchanger. The exhaust gas from the engine is permitted to pass through either the heat exchanger or through the environment by using a one-way irreversible system valve. Gear pump

Table 1. Specifications of the Diesel engine

Type of engine	Single cylinder 4-stroke water cooled Diesel engine
Make	Kirloskar make
Bore	80 mm
Stroke	110 mm
Rated power	7.4 kW
Speed	1500 rpm

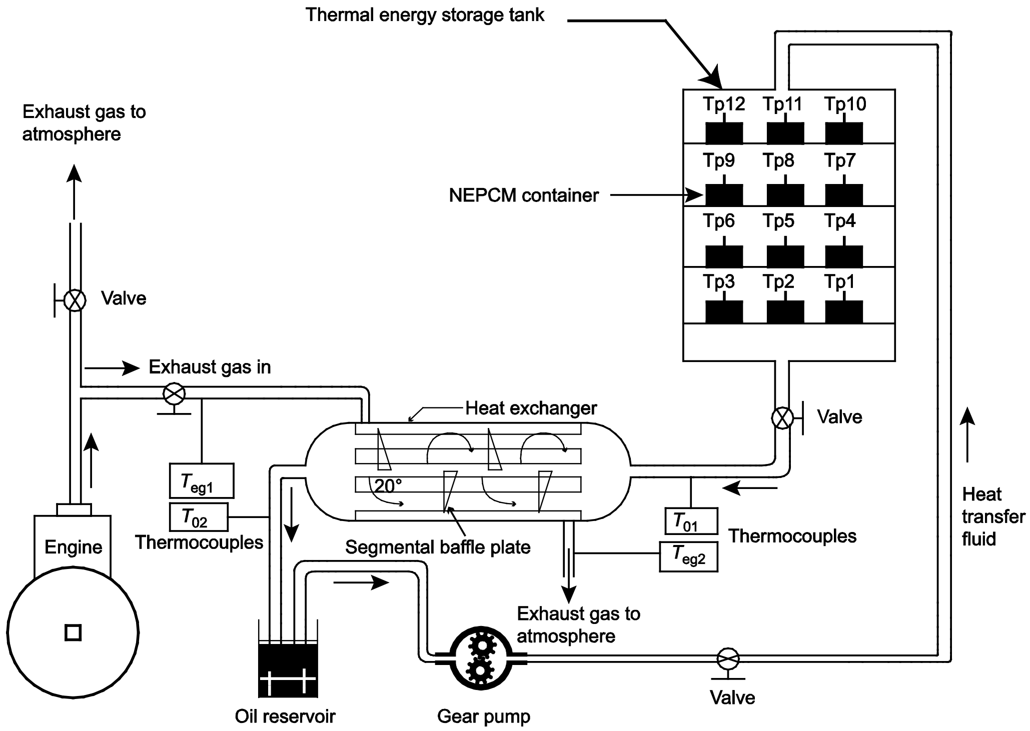

Figure 1. Schematic diagram of experimental set-up

helps to circulate in closed loop Balmerol prototherm medium heat transfer oil, to pass through the tube side of the heat exchanger and thermal storage system [23].

Heat exchanger design

A triangular finned shell and tube heat exchanger is used as the heat energy recovery system; the cylindrical shell is made of mild steel and tubes are made up of Cu. The exhaust gas and Balmerol prototherm medium heat transfer oil are allowed to pass through the shell and tube side of the heat exchanger. Thermophysical properties of the Balmerol prototherm medium heat transfer oil are shown in tab. 2. The shell and tube heat exchanger is fabricated to the following dimensions: outer radius, wall thickness, and length of shell are 161.5, 6, and 500 mm, respectively. Also, the outer radius and wall thickness of tubes are 6 mm and 2.5 mm, respectively, with 36 tubes. Four longitudinal Cu triangular fins of 6 mm height and 2 mm width are attached to each Cu tube at equal intervals. Three aluminum segmental baffles with 50% cut and 20° baffle angle are attached to the tubes at 177.6 mm spacing. The heat exchanger and connecting pipelines are well insulated by glass wool fiber with an aluminum shield to avoid heat leakage to the atmosphere. The dimensions of triangular finned shell and tubes are presented in tab. 3. Figure 2 shows the customized design of triangular finned shell and tube heat exchanger with baffle angle. The K-type thermocouples are placed at the inlet and outlet of the heat exchanger in the heat transfer fluid (HTF) and exhaust gas pipelines. The locations of the thermocouples are also shown in fig. 2. A flow meter is used to measure the flow rate of HTF and a gear pump is used to circulate HTF through the TES tank.

Table 2. Thermophysical properties of the Balmerol prototherm medium heat transfer oil

Properties	Balmerol prototherm medium heat transfer oil
Specific heat, C_p at 300 °C [kJkg^{-1}°C^{-1}]	3.22
Thermal conductivity, K [Wm^{-1}°C^{-1}]	0.11
Kinematic viscosity at 40 °C [m^{2}s^{-1}]	32·10^6
Dynamic viscosity at 40 °C [Pa·s]	0.0308

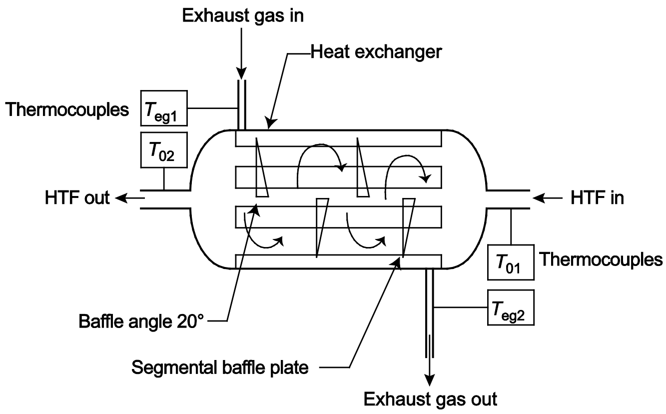

Figure 2. Customized design of triangular finned shell and tube heat exchanger with baffle at 20°

Thermal storage system

Steel plate is rolled to make TES tank in the shape of a cylinder with the dimensions of inner radius 225 mm and height 720 mm. The cylindrical TES tank has NEPCM in the encapsulated small stainless steel cylindrical container of radius 40 mm and height 100 mm. The TES tanks consist of 48 small stainless steel cylindrical containers, which are uniformly arranged in a four-layer structure using a mild steel stand having a wire-mesh. One-

Table 3. Geometry parameters of finned shell and tube heat exchanger

Shell side parameters		Fin parameters	
Type	E type	Type	Longitudinal triangular fin
Material	Mild steel	Material	Copper
Outer radius	161.5 mm	Thickness	2 mm
Wall thickness	6 mm	Height	6 mm
Length	500 mm		
Tube parameters		**Baffle parameters**	
Type	Finned tube	Baffles	50% cut baffles
Material	Copper	No of baffles	3
Outer radius	6 mm	Baffle angle	20°
Wall thickness	1.5 mm	Baffle spacing	177.6 mm
No. of tubes inside the shell	36	Baffle material	Aluminium
Type of tube layout	Square layout	Type of insulation used	Glass wool, covered with aluminum cladding
Type of tube arrangement	In line arrangement		
Transverse pitch	37.5 mm		
Longitudinal pitch	37.5 mm		

-fourth of the area is reserved by NEPCM container and the rest of the space is reserved by Balmerol prototherm medium heat transfer oil as sensible heat storage medium. The total weight of PCM with nanoparticles in the 48 containers is 15 kg and each capsule has 320 g of NEPCM. The geometrical parameters and the heat energy storage capacity of the storage tank are given in tab. 4. The total weight of Balmerol prototherm medium heat transfer oil in TES tank is 55 kg stored as sensible heat energy. The K-type thermocouples are used to measure the temperatures at various locations in TES tank. Twelve thermocouples are connected with NEPCM containers in four uniform horizontal layers, as shown in fig. 1. Three thermocouples are connected uniformly in each layer at different locations.

Table 4. Geometry parameters and heat storage capacity of the TES tank

TES parameters			
Radius	225 mm	Volume	0.115 m^3
Height	720 mm	Material	Stainless steel
Cylindrical container parameters			
Radius	40 mm	Volume of HTF in the storage tank	0.0908 m^3
Height	100	Mass of the paraffin and CuO nanoparticles	15 kg
Number of cylindrical container	48	Mass of the paraffin	14.85 kg
Material	Stainless steel	Mass of the CuO nanoparticles	0.15 kg
Volume	$5.03 \cdot 10^{-4}$ m^3	Mass of the HTF in the storage tank	55 kg
Volume of PCM and nanoparticles in the cylindrical container	$5.03 \cdot 10^{-4}$ m^3		

The NEPCM play a major role in the improvement of heat transfer execution of PCM in a thermal storage system. In order to make a consistent NEPCM, appropriate mixing and stabilization of the nanoparticles with the base PCM are required. The CuO nanoparticles and paraffin wax are mixed together using a magnetic stirrer for half an hour at the temperature of 60 °C. After that, it is dispersed by an ultrasonic vibrator for 3 hours to get stable suspension and homogeneity. Figures 3-5 represent the melting/freezing temperatures and the potential of latent heat energy of 20 mg of the CuO nanoparticles, paraffin wax, and mixture of paraffin wax with CuO nanoparticles, which are obtained by differential scanning calorimetry under a constant stream of nitrogen gas. Differential scanning calorimeter (DSC) measurements are carried out at a heating/cooling rate of 10 °C per minute and a temperature range of 0-110 °C for paraffin wax, of 0-1200 °C for CuO nanoparticles, and 35-90 °C for paraffin wax with CuO nanoparticles. The ranges of accuracy of enthalpy and temperature are estimated to be ±0.5% and ±0.2 °C, respectively. The local increase and decrease in DCS curve indicate the phase change processes. The latent heat is obtained from the area under the peak of the phase change curve per 20 mg. scanning electron microscopy (SEM) image of the paraffin with the CuO nanoparticle is shown in fig. 6. The SEM analysis test result displays the unvarying particle size and globular appearance of the nanoparticle. The nanocomposite PCM are uniformly dispersed in paraffin structure with particle size, paraffin wax mix with CuO.

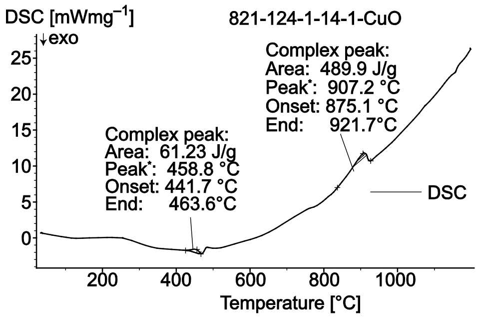

Figure 3. The heating and freezing curves by differential scanning calorimeter of CuO

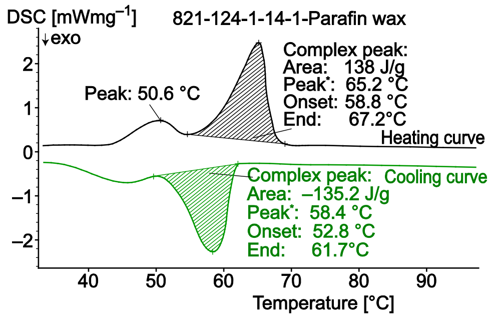

Figure 4. The heating and freezing curves by differential scanning calorimeter of paraffin wax

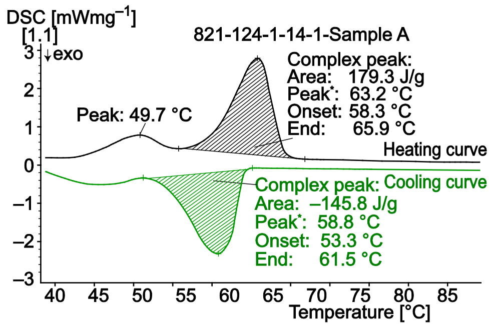

Figure 5. The heating and freezing curves by differential scanning calorimeter of paraffin wax with CuO (5% of CuO for 20 mg of paraffin wax)

Experimental methodology

Experiments were performed for the exhaust heat recovery using triangular finned shell and tube heat exchanger and TES tank from the Diesel engine at various loads supplied to the engine. Initially at any load condition, the exhaust gas is permitted to pass through the

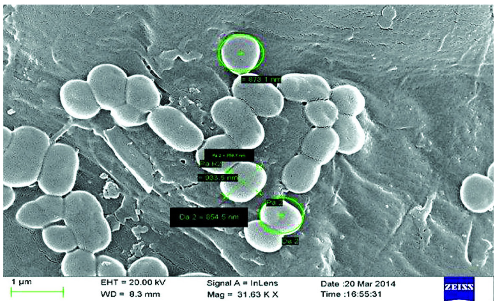

Figure 6. The SEM result of paraffin with CuO

atmosphere by using a valve to protect the tube from carbon deposition. After 10 minutes from the start of the engine, the atmosphere valve is closed and the heat exchanger valve is opened, so that the exhaust gas flows through the shell side of the heat exchanger; this ensures HTF circulates smoothly through the heat exchanger. A tachometer is used to measure the constant speed of the engine and make sure that the rated speed of 1500 rpm is maintained. A U-tube manometer is used to measure the mass flow rate of engine inlet atmospheric air by observing the pressure variation in an orifice meter. Experimental tests were carried out at four varying load conditions with equal intervals from 25% to full load condition. The HTF is passed through the tube side of the heat exchanger to get its higher heat transfer coefficient when compared to the exhaust gas from the engine. The NEPCM is used to store the latent heat in TES system. The temperature readings are taken at equal intervals with respect to the height of TES tank and inlet and outlet of the heat exchanger in HTF and exhaust gas pipelines.

Results and discussion

The temperature distribution of HTF and exhaust gas for various load conditions of the Diesel engine is studied in detail. In the present study, the HTF is circulated in the tube side of a triangular finned shell and tube heat exchanger with aluminum segmental baffles with 50% cut at 20° baffle angle and HTF in closed loop transfer accumulates heat energy in the TES tank with its packed NEPCM mounted inside cylindrical container for recovering the maximum possible heat energy from the exhaust gas of the Diesel engine.

Performance of heat recovery heat exchanger

The temperature observations of the exhaust gas and HTF at the inlet and outlet of the heat recovery heat exchanger (HRHE) with respect to time are shown in fig. 7 for varying engine load conditions from 25% to full load.

The temperature of exhaust gas of the Diesel engine reaches the steady-state within 5 minutes in all loads. However; in the present work the temperature of the exhaust gas at the inlet of HRHE reaches the steady-state after an interval of 25 minutes and this is because of thermal inertia due to insulation of engine exhaust pipe. When the engine load increases, simultaneously the temperature of the exhaust gas also increases due to its higher heat release from the Diesel engine. At all loads, it is observed from HTF and the exhaust gas outlet temperature variation that the temperature increases at the beginning and the slope decreases when the temperature of HTF attains approximately 60 °C and further increases at a higher rate after a certain interval of time. At 25% load a near constant temperature around 60 °C is observed for a longer duration and this duration decreases with increase in load. Figure 7 shows that there is a maximum temperature drop in the exhaust gas at all times and the increase in temperature of HTF is very low since the heat capacity of HTF ($\dot{m}_{\mathrm{HTF}}C_{p,\mathrm{HTF}}$) is much higher than the heat capacity of the exhaust gas ($\dot{m}_{\mathrm{eg}}C_{p,\mathrm{eg}}$). Figure 7 shows the comparison between the temperature difference of HTF and exhaust gas at the inlet and outlet of the custom designed HRHE and that studied by Pandiyarajan *et al.* [23]. From the figures, it is

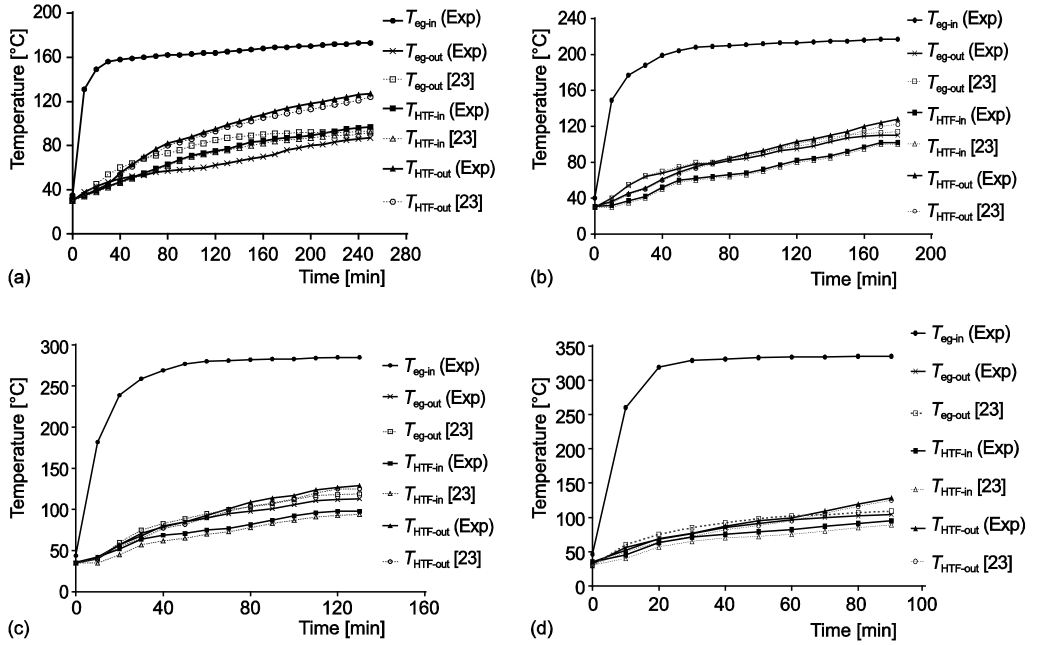

Figure 7. Temperature variation of the exhaust gas and the HTF at the inlet and outlet of the HRHE at various loads: (a) 25% load, (b) 50% load, (c) 75% load, and (d) full load

also observed that in all the four loads the exhaust gas temperature of the engine is very low at the outlet of HRHE using triangular finned surface shell and tube heat exchanger with segmental baffles at 20° with Balmerol prototherm medium heat transfer oil compared to Pandiyarajan *et al.* [23]. Moreover, the temperature of HTF in the outlet of HRHE is nearly 4.27% more than in [23] due to custom design of heat exchanger and high thermal conductivity of HTF. From the previous discussion, it is also concluded that the effectiveness of the customized heat exchanger is more than 99% after completion of the testing in all conditions.

Figure 8 shows the deviation of the heat extraction rate, Q_{eg}, from the exhaust gas through the HRHE which was determined using eq. (1)

$$Q_{eg} = \dot{m}_{eg} C_{p,eg} (T_{eg1} - T_{eg2}) \tag{1}$$

where $\dot{m}_{eg}$ is the mass flow rate of the exhaust gas, T_{eg1}, T_{eg2} are the exhaust gas temperature at the inlet and outlet of HRHE, respectively.

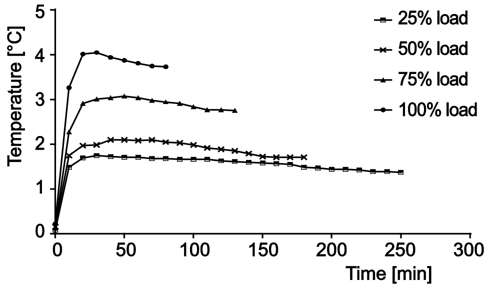

Figure 8. Heat extraction rate from exhaust gas at different load conditions

The maximum heat extraction rate available is 4.04 kW at the full load condition of the engine because of very high heat release rate when compared with other engine load conditions. For all loads, when the time increases the heat transfer rate decreases because of the continuously increasing temperature of HTF at the inlet of HRHE which minimizes the mean temperature variation between the exhaust gas and HTF.

Performance of the thermal storage system

The performance of the thermal storage system is examined by the temperature variation of NEPCM for various load conditions.

Variation of NEPCM temperatures

Figure 1 shows the schematic diagram of the experimental set-up. The temperature distributions are measured inside TES tank at position Tp1 to Tp12 as shown in fig. 1 with respect to time for varying engine load conditions – from 25% load to full load, which is discussed in this section. The average temperature variations of NEPCM at the four layers of TES tank with respect to time are shown in fig. 9 for varying load conditions. It is observed from the figures that because of sensible heat, there is an increase in the temperature of HTF which is high at the starting of the charging process when compared with the temperature of NEPCM in the containers. While the temperature of NEPCM is nearly 70 °C, the sensible heat of HTF is less than the latent heat of NEPCM. Owing to the high thermal conductivity of the CuO nanoparticles, the phase change of NEPCM occurs for a short interval of time. The temperature of NEPCM increases in a small interval of time when the load increases, due to the high temperature of the sensible heat of HTF. There exists a very small temperature difference between the layers. The temperature of NEPCM in the fourth layer is higher than the other layers due to HTF stored at the bottom of the tank. The third layer attains the temperature of the fourth layer only after the melting process is completed in the fourth layer. The melting process of NEPCM in the first layer is faster than the second layer due to the hot HTF which enters at the top of TES tank. The temperature order of the layers in TES tank is: fourth, third, first, and second.

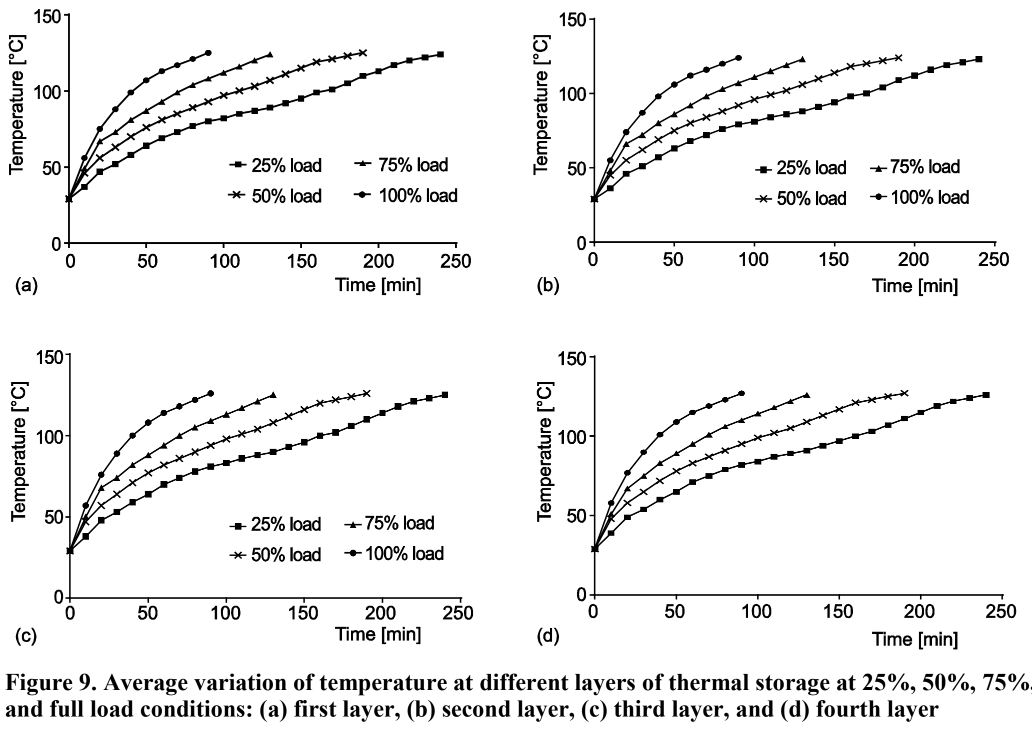

Figure 9. Average variation of temperature at different layers of thermal storage at 25%, 50%, 75%, and full load conditions: (a) first layer, (b) second layer, (c) third layer, and (d) fourth layer

The thermophysical properties of NEPCM (*i. e.* density and specific heat) and heat energy stored in NEPCM were determined using eqs. (2)-(4)

The NEPCM density, ρ_{NEPCM}, was calculated from eq. (2):

$$\rho_{\text{NEPCM}} = (1-\varphi)\rho_{\text{PCM}} + \varphi\rho_{\text{s}} \tag{2}$$

The NEPCM specific heat, $C_{p,\text{NEPCM}}$, was calculated from eq. (3):

$$C_{p,\text{NEPCM}} = \frac{(1-\varphi)(\rho C_p)_{\text{PCM}} + \varphi(\rho C_p)_{\text{s}}}{\rho_{\text{NEPCM}}} \tag{3}$$

Heat energy stored in NEPCM, Q_{NEPCM}, was obtained by using eq. (4):

$$Q_{\text{NEPCM}} = m_{\text{NEPCM}} C_{p,\text{NEPCM}} \Delta T_{\text{NEPCM}} + m_{\text{NEPCM}} L_{\text{NEPCM}} \tag{4}$$

The total heat energy stored in TES tank using NEPCM is 23,913 kJ in which the heat energy stored in HTF is 17,356 kJ with a temperature rise of 98 °C (127-29 °C) and heat energy stored in NEPCM is 6,557 kJ. It is seen from fig. 9 that the time required to change the phase of NEPCM is 40 and 10 minutes at the fourth layer of the 25% and 100% load. Similarly, the time required to change NEPCM is 45 and 12 minutes at the first layer of the 25% and 100% load. The NEPCM reached the phase change temperature at a very short interval of time for the maximum load condition due to high thermal conductivity of the CuO nanoparticles. The experiments were conducted till the temperature inside TES tank attains 127 °C during the charging process for all loads. When the storage tank attains 127 °C, the total heat energy stored in the storage tank is 23,913 kJ with respect to the environment. Although the heat energy stored is the same at all the load conditions, it is observed that the duration of charging is 250 minutes at 25% load and it decreases to 190 min, 130 min, and 90 minutes for 50%, 75% and full load conditions, respectively. This shows that there is a variation in the charging rate.

The charging rate is defined as the average rate at which the heat is supplied to TES tank at a particular load. It is the ratio of the total heat energy stored in TES tank to the duration of charging and is evaluated using eq. (5):

$$Q_{\text{cr}} = \frac{(m_{\text{HTF}} C_{p,\text{HTF}} \Delta T_{\text{HTF}}) + (m_{\text{NEPCM}} C_{p,\text{NEPCM}} \Delta T_{\text{NEPCM}}) + m_{\text{NEPCM}} L_{\text{NEPCM}}}{\Delta t_{\text{C}}} \quad [\text{kW}] \tag{5}$$

The faster charging at higher loads reduces the losses encountered during the charging process. Figure 10 shows the charging rate at various load conditions. It is seen from the figure that the charging rate increases with increase in load as the time required to charge the same quantity of heat energy in TES tank decreases from 250 to 90 minutes when the load increases.

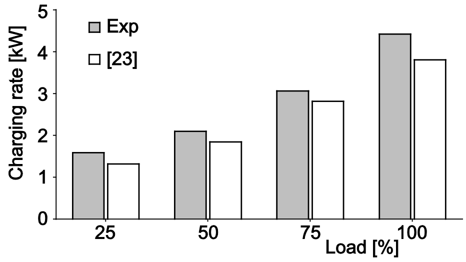

Figure 10. Charging rate at various loads

This is due to increase in exhaust gas temperature achieved at higher loads within a short duration after the start of the engine. This provided the higher temperature difference for heat transfer during the charging process at higher loads. Further it is observed from fig. 10 that the charging rate of NEPCM in TES tank for all the loads is comparatively more than that studied by Pandiyarajan *et al.* [23]. Hence, the loss encountered during charging is less by using NEPCM in TES tank.

Conclusions

The heat energy of the exhaust gas in the Diesel engine can be recovered and stored successfully by using triangular finned shell and tube heat exchanger and TES tank with NEPCM. The sensible heat can be enhanced using Balmerol protootherm medium heat transfer oil and the effectiveness of the heat exchanger can be enhanced using custom designed triangular finned shell and tube heat exchanger. In the conventional PCM, the thermal conductivity is low, which can be increased by using NEPCM.

In the present work, the custom designed triangular finned shell and tube heat exchanger and NEPCM based TES tank of capacity 23,913 kJ were fabricated and tested by integrating them with a Diesel engine of capacity 7.4 kW. The temperature of the exhaust gas and HTF during charging process at the inlet and outlet of the customized HRHE with respect to time are discussed. It is observed from the experimental results that the heat extraction rate is 4.04 kW in full load condition of the engine. The effectiveness of the customized heat exchanger is more than 99% after completion of the testing in all the loads. Experimental results show that the temperature of Balmerol protootherm medium heat transfer oil in outlet of HRHE is nearly 4.27% more than the one studied by Pandiyarajan *et al.* [23]. The charging rate of NEPCM in TES tank at higher loads is 4.43 kW and the value decreases with respect to the load. It is concluded that NEPCM has the greatest potential for energy storage applications in WHR from the Diesel engine.

Nomenclature

C_p – specific heat at constant pressure, [Jkg^{-1} °C^{-1}]
K – thermal conductivity, [Wm^{-1} °C^{-1}]
L – latent heat fusion, [Jkg^{-1}]
m – mass, [kg]
$\dot{m}$ – mass flow rate, [kgs^{-1}]
Q – heat extraction rate, [kW]
T_{eg1} – exhaust gas temperature at HRHE inlet, [°C]
T_{eg2} – exhaust gas temperature at HRHE outlet, [°C]
ΔT – change in temperature, [°C]
Δt_c – duration of charging, [s]

Acronyms

DSC – differential scaning calorimeter
HRHE – heat recovery heat exchanger
HTF – heat transfer fluid
NEPCM – nanoenhanced phase change material
PCM – phase change material
TES – thermal energy storage

Greek symbols

ρ – density, [kgm^{-3}]
φ – volume fraction of nanoparticle

Subscripts

eg – exhaust gas
s – solid (nanoparticle)

References

[1] Mittal, A., *et al.*, A Refrigeration System for an Automobile Based on Vapor Absorption Refrigeration Cycle Using Waste Heat Energy from the Engine, *International Journal of Engineering Sciences & Research Technology*, *4* (2015), 4, pp. 591-598
[2] Yu, C., Chau, K. T., Thermoelectric Automotive Waste Heat Energy Recovery Using Maximum Power Point Tracking, *Energy Conversion and Management*, *50* (2009), 6, pp. 1506-1512
[3] He, M., *et al.*, A Combined Thermodynamic Cycle Used for Waste Heat Recovery of Internal Combustion Engine, *Energy*, *36* (2011), 12, pp. 6821-6829
[4] Wang, E. H., *et al.*, Study of Working Fluid Selection of Organic Rankine Cycle (ORC) for Engine Waste Heat Recovery, *Energy*, *36* (2011), 5, pp. 3406-3418
[5] Heywood, J., *International Combustion Engine Fundamentals*, McGraw-Hill Education, New York, USA, 1988

[6] Saidur, R., *et al.*, Energy and Emission Analysis for Industrial Motors in Malaysia, *Energy Policy*, *37* (2009), 9, pp. 3650-3658
[7] Hasanuzzaman, M., *et al.*, Energy Savings and Emissions Reductions for Rewinding and Replacement of Industrial Motor, *Energy*, *36* (2011), 1, pp. 233-240
[8] Chammas, R. E., Clodic, D., Combined Cycle for Hybrid Vehicles, SAE Int. publication, 2005-01-1171, 2005
[9] Ozcan, H., Soylemeze, M. S., Thermal Balance of a LPG Fuelled, Four Stroke SI Engine with Water Addition, *Energy Conversion and Management*, *47* (2006), 5, pp. 570-581
[10] Sachdeva, R. C., *Fundamentals of Engineering Heat and Mass Transfer*, Wiley Eastern Limited, New York, USA, 1992
[11] Hatami, M., *et al.*, A Review of Different Heat Exchangers Designs for Increasing the Diesel Exhaust Waste Heat Recovery, *Renewable and Sustainable Energy Reviews*, *37* (2014), Sept., pp. 168-181
[12] Bari, S., Hossain, S. N., Waste Heat Recovery from a Diesel Engine Using Shell and Tube Heat Exchanger, *Applied Thermal Engineering*, *61* (2013), 2, pp. 355-363
[13] Morcos, V. H., Performance of Shell-and-Dimpled-Tube Heat Exchangers for Waste Heat Recovery, *Heat Recovery Systems CHP*, *8* (1988), 4, pp. 299-308
[14] Jegadheeswaran, S., Pohekar, S. D., Performance Enhancement in Latent Heat Thermal Storage System: A review, *Renewable and Sustainable Energy Reviews*, *13* (2009), 9, pp. 2225-2244
[15] Hatami, M., *et al.*, Numerical Study of Finned Type Heat Exchangers for ICEs Exhaust Waste Heat Recovery, *Case Studies in Thermal Engineering*, *4* (2014), Nov., pp. 53-64
[16] Ismail, K. A. R., *et al.*, Numerical and Experimental Study on the Solidification of PCM Around a Vertical Axially Finned Isothermal Cylinder, *Applied Thermal Engineering*, *21* (2001), 1, pp. 53-77
[17] Taher, F., *et al.*, Baffle Space Impact on the Performance of Helical Baffle Shell and Tube Heat Exchangers, *Applied Thermal Engineering*, *44* (2012), Nov., pp. 143-159
[18] Elias, M. M., *et al.*, Effect of Different Nanoparticle Shapes on Shell and Tube Heat Exchanger Using Different Baffle Angles and Operated with Nanofluid, *International Journal of Heat and Mass Transfer*, *70* (2014), Mar., pp. 289-297
[19] Hosseini, M. J., *et al.*, A Combined Experimental and Computation Study on the Melting Behavior of a Medium Temperature Phase Change Storage Material Inside Shell and Tube Heat Exchanger, *International Communications in Heat and Mass Transfer*, *39* (2012), 9, pp. 1416-1424
[20] Agyenim, F., *et al.*, A Review of Materials, Heat Transfer and Phase Change Problem Formulation for Latent Heat Thermal Energy Storage Systems (LHTESS), *Renewable and Sustainable Energy Reviews*, *14* (2010), 2, pp. 615-628
[21] Sharma, A., *et al.*, Review on Thermal Energy Storage with Phase Change Materials and Applications, *Renewable and Sustainable Energy Reviews*, *13* (2009), 2, pp. 318-345
[22] Cunha, J., Eames, P., Thermal Energy Storage for Low and Medium Temperature Applications Using Phase Change Materials – A review, *Applied Energy*, *177* (2016), Sept., pp. 227-238
[23] Pandiyarajan, V., *et al.*, Experimental Investigation on Heat Recovery from Diesel Engine Exhaust Using Finned Shell and Tube Heat Exchanger and Thermal Storage System, *Applied Energy*, *88* (2011), 1, pp. 77-87
[24] Nallusamy, N., *et al.*, Experimental Investigation on a Combined Sensible and Latent Heat Storage System Integrated with Constant/Varying (Solar) Heat Sources, *Renewable Energy*, *32* (2007), 7, pp. 1206-1227
[25] Medrano, M., *et al.*, Experimental Evaluation of Commercial Heat Exchangers for Use as PCM Thermal Storage Systems, *Applied Energy*, *86* (2009), 10, pp. 2047-2055
[26] Hosseinizadeh, S. F., *et al.*, Numerical Investigations of Unconstrained Melting of Nano-Enhanced Phase Change Material (NEPCM) Inside a Spherical Container, *International Journal of Thermal Sciences*, *51* (2012), Jan., pp. 77-83
[27] Ranjbar, A. A., *et al.*, Numerical Heat Transfer Studies of a Latent Heat Storage System Containing Nano-Enhanced Phase Change Material, *Thermal Science*, *15* (2011), 1, pp. 169-181
[28] Jesumathy, S., *et al.*, Experimental Study of Enhanced Heat Transfer by Addition of CuO Nanoparticle, *Heat Mass Transfer*, *48* (2012), 6, pp. 965-978

Paper submitted: April 26, 2016
Paper revised: August 12, 2016
Paper accepted: August 22, 2016